Supplement of Atmos. Chem. Phys., 22, 11543–11555, 2022
https://doi.org/10.5194/acp-22-11543-2022-supplement

Atmospheric Chemistry and Physics
Open Access
EGU

Supplement of

Atmospheric oxidation mechanism and kinetics of indole initiated by ·OH and ·Cl: a computational study

Jingwen Xue et al.

Correspondence to: Fangfang Ma (maff@dlut.edu.cn) and Hong-Bin Xie (hbxie@dlut.edu.cn)

Contents

Tunneling effects

For the reactions involving H-abstraction or H-shift, tunneling effects could influence their reaction rate constants and branching ratios of products. To probe the tunneling effects, reaction rate constants (k) of bimolecular H-abstraction pathways and unimolecular H-shift pathways involved in the key reaction pathways and branching ratios (Γ) of important species (intermediates (IM_{1-7}, IM_{2-5} and IM_{2-6}), products (P_{2-10}, $P_{1-7-4-1}$), organonitrates (and alkoxy radicals, NO-P_3 and NO-P_4), hydroperoxide (HO_2-P_3, and HO_2-P_4)) without tunneling effects were calculated at 298 K and 1 atm. The calculated data are shown in Table S1. It can be noted that all the values of k without the tunneling effects are at least one (up to three) order of magnitude lower than the corresponding values with tunneling effects, indicating that tunneling effects can significantly increase k values of the important reaction pathways. In addition, the tunneling effects have various effects on the branching ratios of important species. The tunneling effects increase the yields of P_{2-10}, and $P_{1-7-4-1}$, almost have no effect on the yields of IM_{1-7}, IM_{2-6}, NO-P_4 and HO_2-P_4 and reduce the yields of IM_{2-5}, NO-P_3 and HO_2-P_3.

Table S1. Calculated reaction rate constants (k) of important unimolecular H-shift/bimolecular H-abstraction pathways and branching ratios (Γ) of main products with and without considering tunneling effects at 298 K and 1 atm .

Pathways	k		Species	Γ	
	Tun*	NoTun#		Tun*	NoTun#
$R_1 \rightarrow P_{1-10}$	1.7×10^{-15} cm^3 molecule^{-1} s^{-1}	1.1×10^{-16} cm^3 molecule^{-1} s^{-1}	IM_{1-7}	77.4%	77.9%
			IM_{2-5}	31.4%	34.3%
$R_2 \rightarrow P_{2-10}$	4.5×10^{-11} cm^3 molecule^{-1} s^{-1}	8.7×10^{-12} cm^3 molecule^{-1} s^{-1}	IM_{2-6}	45.5%	50.1%
			P_{2-10}	23.1%	15.6%
IM_{1-7}-4OO-*s*$\rightarrow$ IM_{1-7}-4OO-OH-*s*	1.2×10^{-2} s^{-1}	5.5×10^{-3} s^{-1}	$P_{1-7-4-1}$	6.4%	3.1%
			NO-P_3	67.3%	70.6%
IM_{2-5}-6OO-*a*$\rightarrow$ IM_{2-5}-6OO-C5H-*a*	7.6×10^{-4} s^{-1}	2.3×10^{-7} s^{-1}	HO_2-P_3	24.9%	26.1%
			NO-P_4	72.4%	73.0%
			HO_2-P_4	26.8%	27.0%

*Tunneling effects were taken into account when calculating the reaction rate constants.

#Tunneling effects were not taken into account when calculating the reaction rate constants.

Table S2. Values of T_1 diagnostics for the intermediates and transition states involved in the key reaction pathways in the CCSD(T)/6-31+G(d') calculations within the CBS-QB3 scheme.

Species	T_1 diagnostics	Species	T_1 diagnostics
$TS_{1\text{-}7}$	0.039	$IM_{1\text{-}7}$	0.033
$TS_{2\text{-}5}$	0.033	$IM_{2\text{-}5}$	0.031
$TS_{2\text{-}6}$	0.034	$IM_{2\text{-}6}$	0.031
$TS_{2\text{-}10}$	0.028	C_8H_6N	0.039
$TS_{3\text{-}2}$	0.038	$IM_{1\text{-}7}$-4OO-*s*	0.020
$TS_{3\text{-}2'}$	0.037	$IM_{1\text{-}7}$-4OO-*a*	0.020
$TS_{3\text{-}2\text{-}4}$	0.037	$IM_{1\text{-}7}$-4OO-NH-*s*	0.031
$TS_{3\text{-}2\text{-}7}$	0.027	$IM_{1\text{-}7}$-4OO-OH-*s*	0.035
$TS_{4\text{-}3}$	0.035	$IM_{2\text{-}5}$-6OO-*s*	0.020
$TS_{4\text{-}3'}$	0.036	$IM_{2\text{-}5}$-6OO-*a*	0.020
$TS_{4\text{-}3'\text{-}7}$	0.032	$IM_{2\text{-}5}$-6OO-C5H-*a*	0.029
$TS_{5\text{-}2}$	0.037	$IM_{2\text{-}6}$-5OO-*s*	0.020
$TS_{5\text{-}2'}$	0.038	$IM_{2\text{-}6}$-5OO-*a*	0.020
$TS_{5\text{-}2'\text{-}1}$	0.031	$IM_{2\text{-}6}$-52OO-*a*	0.023
$TS_{6\text{-}2}$	0.036	C_8H_6N-4OO-*s*	0.021
$TS_{6\text{-}2'}$	0.036	C_8H_6N-4OO-*a*	0.021
$TS_{6\text{-}2\text{-}3}$	0.043	C_8H_6N-43OO-*s*	0.036
$TS_{6\text{-}2'\text{-}3}$	0.043	C_8H_6N-43OO-*a*	0.036

45

Table S3. Polarizabilities (α) and the first ionization potentials (I) used in the long-range transition state theory.

Species	α/a_0^3	I/(eV)
C_8H_7N (indole)	105.62*	7.74*
$\cdot C_8H_6N$ ($P_{1\text{-}10}/P_{2\text{-}10}$)	106.58*	8.08*
$\cdot C_8H_6N$ ($P_{1\text{-}11}/P_{2\text{-}11}$)	104.79*	8.29*
$\cdot C_8H_6N$ ($P_{1\text{-}12}/P_{2\text{-}12}$)	104.90*	8.04*
$\cdot C_8H_6N$ ($P_{1\text{-}13}/P_{2\text{-}13}$)	104.49*	7.68*
$\cdot C_8H_6N$ ($P_{1\text{-}14}/P_{2\text{-}14}$)	103.25*	8.13*
$\cdot C_8H_6N$ ($P_{1\text{-}15}/P_{2\text{-}15}$)	103.47*	7.80*
$\cdot C_8H_6N$ ($P_{1\text{-}16}/P_{2\text{-}16}$)	104.00*	7.62*
·OH	8.26#	15.24#
$H_2O\cdot$	10.60#	14.71#
·Cl	14.71#	12.97#
HCl	16.97#	12.74#

* α and I were calculated at BLYP/def2-QZVPD and CBS-QB3//M06-2X/6-31+G(d,p) level of theory, respectively, which have been used in our previous studies.[1-4]

Obtained from the NIST database [5]

Table S4. Lennard-Jones parameters of the intermediates for various reactions used in the MultiWell or MESMER simulations.

Reactions	σ/(Å)	ε/(K)
Indole + ·OH	6.4	685
Indole + ·Cl	6.5	619
$IM_{1\text{-}7} + O_2$	6.6	739
$IM_{2\text{-}5} + O_2$	6.7	673
$IM_{2\text{-}6} + O_2$	6.7	673
$C_8H_6N + O_2$	6.4	635

Table S5. NBO charge distribution for all the pre-reactive complexes of the indole + ·Cl reaction.

Species	Atoms	Number	Natural Charge
Indole 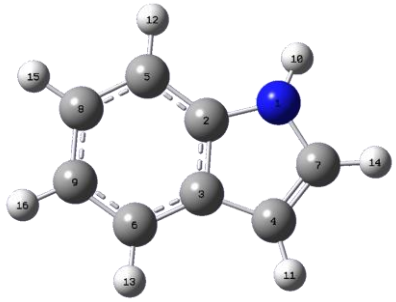	N	1	-0.596
	C	2	0.143
	C	3	-0.109
	C	4	-0.327
	C	5	-0.274
	C	6	-0.222
	C	7	-0.043
	C	8	-0.255
	C	9	-0.276
	H	10	0.453
	H	11	0.259
	H	12	0.249
	H	13	0.250
	H	14	0.248
	H	15	0.250
	H	16	0.250
$RC_{2\text{-}5}$ 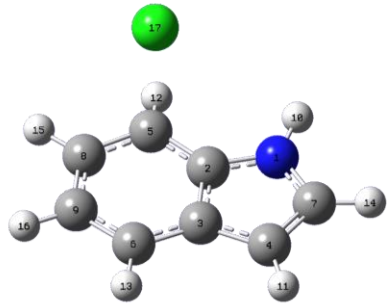	N	1	-0.563
	C	2	0.173
	C	3	-0.127
	C	4	-0.304
	C	5	-0.241
	C	6	-0.141
	C	7	-0.040
	C	8	-0.185
	C	9	-0.286
	H	10	0.466
	H	11	0.265
	H	12	0.294
	H	13	0.256
	H	14	0.256
	H	15	0.266

	H	16	0.261
	Cl	17	-0.350
$RC_{2\text{-}6}$ 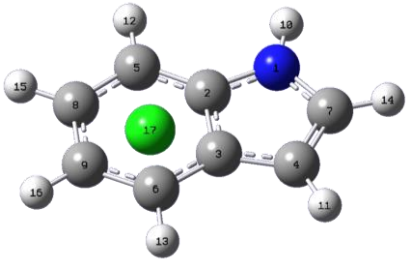	N	1	-0.576
	C	2	0.126
	C	3	-0.087
	C	4	-0.302
	C	5	-0.201
	C	6	-0.199
	C	7	-0.020
	C	8	-0.273
	C	9	-0.193
	H	10	0.459
	H	11	0.270
	H	12	0.254
	H	13	0.293
	H	14	0.255
	H	15	0.260
	H	16	0.267
	Cl	17	-0.334
$RC_{2\text{-}10}$ 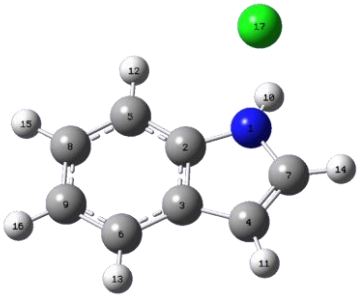	N	1	-0.524
	C	2	0.140
	C	3	-0.099
	C	4	-0.260
	C	5	-0.240
	C	6	-0.215
	C	7	-0.042
	C	8	-0.246
	C	9	-0.252
	H	10	0.484
	H	11	0.267
	H	12	0.263
	H	13	0.257
	H	14	0.265

	H	15	0.257
	H	16	0.256
	Cl	17	-0.310
$RC_{2\text{-}11}$	N	1	-0.578
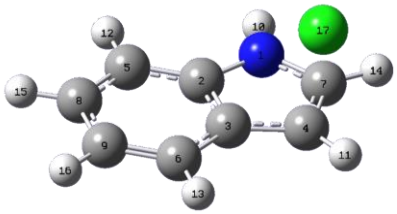	C	2	0.165
	C	3	-0.122
	C	4	-0.221
	C	5	-0.269
	C	6	-0.193
	C	7	0.041
	C	8	-0.228
	C	9	-0.268
	H	10	0.465
	H	11	0.288
	H	12	0.257
	H	13	0.260
	H	14	0.281
	H	15	0.257
	H	16	0.257
	Cl	17	-0.391
$RC_{2\text{-}12}$	N	1	-0.563
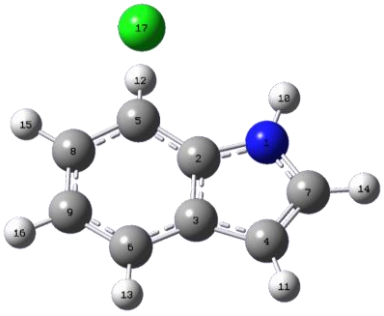	C	2	0.173
	C	3	-0.127
	C	4	-0.304
	C	5	-0.241
	C	6	-0.141
	C	7	-0.040
	C	8	-0.185
	C	9	-0.286
	H	10	0.466
	H	11	0.265
	H	12	0.294
	H	13	0.256

	H	14	0.256
	H	15	0.266
	H	16	0.261
	Cl	17	-0.350
$RC_{2\text{-}13}$	N	1	-0.576
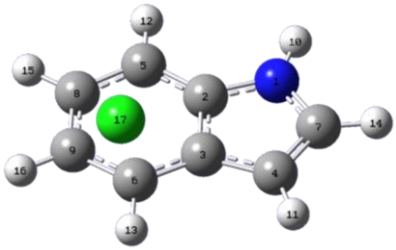	C	2	0.126
	C	3	-0.087
	C	4	-0.302
	C	5	-0.201
	C	6	-0.199
	C	7	-0.020
	C	8	-0.273
	C	9	-0.193
	H	10	0.459
	H	11	0.270
	H	12	0.254
	H	13	0.293
	H	14	0.255
	H	15	0.260
	H	16	0.267
	Cl	17	-0.334
$RC_{2\text{-}14}$	N	1	-0.578
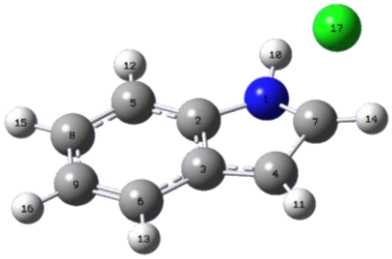	C	2	0.165
	C	3	-0.122
	C	4	-0.221
	C	5	-0.269
	C	6	-0.193
	C	7	0.041
	C	8	-0.228
	C	9	-0.268
	H	10	0.465
	H	11	0.288
	H	12	0.257

	H	13	0.260
	H	14	0.281
	H	15	0.257
	H	16	0.257
	Cl	17	-0.391
$RC_{2\text{-}15}$	N	1	-0.563
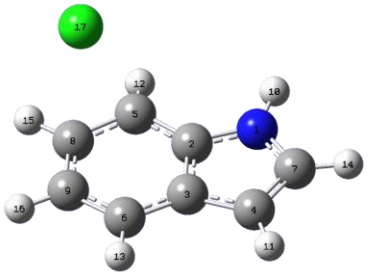	C	2	0.173
	C	3	-0.127
	C	4	-0.304
	C	5	-0.241
	C	6	-0.141
	C	7	-0.040
	C	8	-0.185
	C	9	-0.286
	H	10	0.466
	H	11	0.265
	H	12	0.294
	H	13	0.256
	H	14	0.256
	H	15	0.266
	H	16	0.261
	Cl	17	-0.350
$RC_{2\text{-}16}$	N	1	-0.579
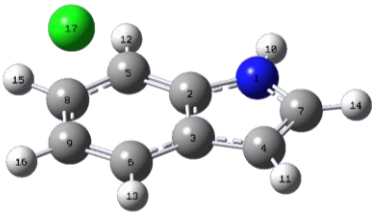	C	2	0.123
	C	3	-0.068
	C	4	-0.323
	C	5	-0.197
	C	6	-0.213
	C	7	-0.006
	C	8	-0.226
	C	9	-0.242
	H	10	0.462
	H	11	0.266

H	12	0.267
H	13	0.258
H	14	0.255
H	15	0.289
H	16	0.264
Cl	17	-0.331

Table S6. Calculated reaction rate constants (*k*) at 298 K and over the pressure range from 0.1 to 1.0 atm of the main reaction pathways for the indole + ·OH/·Cl reactions

Pathways	*k*			
	0.1 atm	**0.4 atm**	**0.7 atm**	**1.0 atm**
Indole + ·OH	7.90×10^{-11} cm^3 $molecule^{-1}$ s^{-1}	7.90×10^{-11} cm^3 $molecule^{-1}$ s^{-1}	7.90×10^{-11} cm^3 $molecule^{-1}$ s^{-1}	7.90×10^{-11} cm^3 $molecule^{-1}$ s^{-1}
Indole + ·Cl	2.91×10^{-10} cm^3 $molecule^{-1}$ s^{-1}	2.91×10^{-10} cm^3 $molecule^{-1}$ s^{-1}	2.91×10^{-10} cm^3 $molecule^{-1}$ s^{-1}	2.91×10^{-10} cm^3 $molecule^{-1}$ s^{-1}
$IM_{1\text{-}7} + O_2$	6.12×10^{-12} cm^3 $molecule^{-1}$ s^{-1}	6.12×10^{-12} cm^3 $molecule^{-1}$ s^{-1}	6.12×10^{-12} cm^3 $molecule^{-1}$ s^{-1}	6.12×10^{-12} cm^3 $molecule^{-1}$ s^{-1}
$IM_{2\text{-}5} + O_2$	6.15×10^{-12} cm^3 $molecule^{-1}$ s^{-1}	6.15×10^{-12} cm^3 $molecule^{-1}$ s^{-1}	6.15×10^{-12} cm^3 $molecule^{-1}$ s^{-1}	6.15×10^{-12} cm^3 $molecule^{-1}$ s^{-1}
$IM_{2\text{-}6} + O_2$	6.10×10^{-12} cm^3 $molecule^{-1}$ s^{-1}	6.10×10^{-12} cm^3 $molecule^{-1}$ s^{-1}	6.10×10^{-12} cm^3 $molecule^{-1}$ s^{-1}	6.10×10^{-12} cm^3 $molecule^{-1}$ s^{-1}
$C_8H_6N + O_2$	6.13×10^{-12} cm^3 $molecule^{-1}$ s^{-1}	6.13×10^{-12} cm^3 $molecule^{-1}$ s^{-1}	6.13×10^{-12} cm^3 $molecule^{-1}$ s^{-1}	6.13×10^{-12} cm^3 $molecule^{-1}$ s^{-1}
$IM_{1\text{-}7}$-4OO-*s*→ $IM_{1\text{-}7}$-4OO-OH-*s*	1.22×10^{-2} s^{-1}	1.22×10^{-2} s^{-1}	1.22×10^{-2} s^{-1}	1.22×10^{-2} s^{-1}
$IM_{2\text{-}5}$-6OO-*a*→ $IM_{2\text{-}5}$-6OO-C5H-*a*	7.65×10^{-4} s^{-1}	7.65×10^{-4} s^{-1}	7.65×10^{-4} s^{-1}	7.65×10^{-4} s^{-1}
$IM_{2\text{-}6}$-5OO-*a*→ $IM_{2\text{-}6}$-52OO-*a*	3.60×10^{-7} s^{-1}	3.60×10^{-7} s^{-1}	3.60×10^{-7} s^{-1}	3.60×10^{-7} s^{-1}
C_8H_6N-4OO-*a/s*→ C_8H_6N-43OO-*a/s*	8.77×10^{-9} s^{-1}	8.77×10^{-9} s^{-1}	8.77×10^{-9} s^{-1}	8.77×10^{-9} s^{-1}

Table S7. Calculated reaction rate constants (*k*) at 298 K and over the energy transfer parameters from 50 to 250 cm^{-1} of the main reaction pathways for the indole + ·OH/·Cl reactions

Pathways	*k*				
	ΔE_d = 50 cm^{-1}	ΔE_d = 100 cm^{-1}	ΔE_d = 150 cm^{-1}	ΔE_d = 200 cm^{-1}	ΔE_d = 250 cm^{-1}
Indole+·OH	7.89×10^{-11} cm^3 $molecule^{-1}$ s^{-1}	7.89×10^{-11} cm^3 $molecule^{-1}$ s^{-1}	7.90×10^{-11} cm^3 $molecule^{-1}$ s^{-1}	7.90×10^{-11} cm^3 $molecule^{-1}$ s^{-1}	7.90×10^{-11} cm^3 $molecule^{-1}$ s^{-1}
Indole+·Cl	2.90×10^{-10} cm^3 $molecule^{-1}$ s^{-1}	2.90×10^{-10} cm^3 $molecule^{-1}$ s^{-1}	2.91×10^{-10} cm^3 $molecule^{-1}$ s^{-1}	2.91×10^{-10} cm^3 $molecule^{-1}$ s^{-1}	2.91×10^{-10} cm^3 $molecule^{-1}$ s^{-1}
$IM_{1\text{-}7}$ + O_2	6.12×10^{-12} cm^3 $molecule^{-1}$ s^{-1}	6.12×10^{-12} cm^3 $molecule^{-1}$ s^{-1}	6.12×10^{-12} cm^3 $molecule^{-1}$ s^{-1}	6.12×10^{-12} cm^3 $molecule^{-1}$ s^{-1}	6.12×10^{-12} cm^3 $molecule^{-1}$ s^{-1}
$IM_{2\text{-}5}$ + O_2	6.15×10^{-12} cm^3 $molecule^{-1}$ s^{-1}	6.15×10^{-12} cm^3 $molecule^{-1}$ s^{-1}	6.15×10^{-12} cm^3 $molecule^{-1}$ s^{-1}	6.15×10^{-12} cm^3 $molecule^{-1}$ s^{-1}	6.15×10^{-12} cm^3 $molecule^{-1}$ s^{-1}
$IM_{2\text{-}6}$ + O_2	6.10×10^{-12} cm^3 $molecule^{-1}$ s^{-1}	6.10×10^{-12} cm^3 $molecule^{-1}$ s^{-1}	6.10×10^{-12} cm^3 $molecule^{-1}$ s^{-1}	6.10×10^{-12} cm^3 $molecule^{-1}$ s^{-1}	6.10×10^{-12} cm^3 $molecule^{-1}$ s^{-1}
C_8H_6N + O_2	6.13×10^{-12} cm^3 $molecule^{-1}$ s^{-1}	6.13×10^{-12} cm^3 $molecule^{-1}$ s^{-1}	6.13×10^{-12} cm^3 $molecule^{-1}$ s^{-1}	6.13×10^{-12} cm^3 $molecule^{-1}$ s^{-1}	6.13×10^{-12} cm^3 $molecule^{-1}$ s^{-1}
$IM_{1\text{-}7}$-4OO-*s*→ $IM_{1\text{-}7}$-4OO-OH-*s*	1.22×10^{-2} s^{-1}	1.22×10^{-2} s^{-1}	1.22×10^{-2} s^{-1}	1.22×10^{-2} s^{-1}	1.22×10^{-2} s^{-1}
$IM_{2\text{-}5}$-6OO-*a*→ $IM_{2\text{-}5}$-6OO-C5H-*a*	7.65×10^{-4} s^{-1}	7.65×10^{-4} s^{-1}	7.65×10^{-4} s^{-1}	7.65×10^{-4} s^{-1}	7.65×10^{-4} s^{-1}
$IM_{2\text{-}6}$-5OO-*a*→ $IM_{2\text{-}6}$-52OO-*a*	3.60×10^{-7} s^{-1}	3.60×10^{-7} s^{-1}	3.60×10^{-7} s^{-1}	3.60×10^{-7} s^{-1}	3.60×10^{-7} s^{-1}
C_8H_6N-4OO-*a/s*→ C_8H_6N-43OO-*a/s*	8.77×10^{-9} s^{-1}	8.77×10^{-9} s^{-1}	8.77×10^{-9} s^{-1}	8.77×10^{-9} s^{-1}	8.77×10^{-9} s^{-1}

Table S8. Calculated branching ratios (*Γ*) at 298 K and over the pressure range from 0.1 to 1.0 atm of the main reaction pathways for the indole + ·OH/·Cl reactions

Species	*Γ*			
	0.1 atm	**0.4 atm**	**0.7 atm**	**1.0 atm**
$IM_{1\text{-}7}$	77.4%	77.4%	77.4%	77.4%
$IM_{2\text{-}5}$	31.4%	31.4%	31.4%	31.4%
$IM_{2\text{-}6}$	45.5%	45.5%	45.5%	45.5%
$P_{2\text{-}10}$	23.1%	23.1%	23.1%	23.1%
$P_{1\text{-}7\text{-}4\text{-}1}$	6.6%	6.5%	6.5%	6.5%
NO-P_3	67.3%	67.3%	67.3%	67.3%
HO_2-P_3	24.9%	24.9%	24.9%	24.9%
NO-P_4	72.4%	72.4%	72.4%	72.4%
HO_2-P_4	26.8%	26.8%	26.8%	26.8%
NO-P_5	72.7%	72.7%	72.7%	72.7%
HO_2-P_5	26.9%	26.9%	26.9%	26.9%
NO-P_6	73.0%	73.0%	73.0%	73.0%
HO_2-P_6	27.0%	27.0%	27.0%	27.0%

Table S9. Calculated branching ratios (Γ) at 298 K and over the energy transfer parameters range from 50 to 250 cm^{-1} of the main reaction pathways for the indole + ·OH/·Cl reactions

Species	Γ				
	ΔE_d = 50 cm^{-1}	ΔE_d = 100 cm^{-1}	ΔE_d = 150 cm^{-1}	ΔE_d = 200 cm^{-1}	ΔE_d = 250 cm^{-1}
IM_{1-7}	77.4%	77.4%	77.4%	77.4%	77.4%
IM_{2-5}	31.4%	31.4%	31.4%	31.4%	31.4%
IM_{2-6}	45.5%	45.5%	45.5%	45.5%	45.5%
P_{2-10}	23.1%	23.1%	23.1%	23.1%	23.1%
$P_{1-7-4-1}$	6.5%	6.5%	6.5%	6.5%	6.5%
NO-P_3	67.3%	67.3%	67.3%	67.3%	67.3%
HO_2-P_3	24.9%	24.9%	24.9%	24.9%	24.9%
NO-P_4	72.4%	72.4%	72.4%	72.4%	72.4%
HO_2-P_4	26.8%	26.8%	26.8%	26.8%	26.8%
NO-P_5	72.7%	72.7%	72.7%	72.7%	72.7%
HO_2-P_5	26.9%	26.9%	26.9%	26.9%	26.9%
NO-P_6	73.0%	73.0%	73.0%	73.0%	73.0%
HO_2-P_6	27.0%	27.0%	27.0%	27.0%	27.0%

Table S10. Calculated spin distribution based on the Mulliken population analysis for main intermediates involved in the indole + ·OH/·Cl reactions.

Species	Atoms	Number	Mulliken atomic spin densities
IM_{1-7} 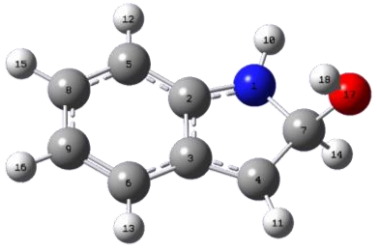	N	1	0.038
	C	2	0.146
	C	3	-0.222
	C	4	0.729
	C	5	-0.111
	C	6	0.287
	C	7	-0.039
	C	8	0.278
	C	9	-0.107
	H	10	-0.002
	H	11	-0.031
	H	12	0.003
	H	13	-0.011
	H	14	0.027
	H	15	-0.013
	H	16	0.003
	O	17	0.021
	H	18	0.003
IM_{2-5} 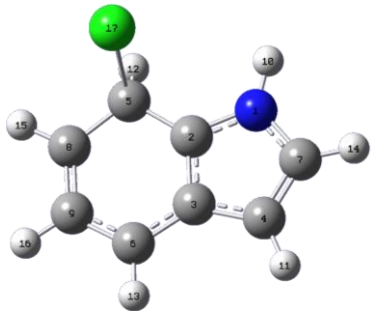	N	1	0.044
	C	2	0.200
	C	3	-0.186
	C	4	0.103
	C	5	-0.061
	C	6	0.573
	C	7	-0.055
	C	8	0.461
	C	9	-0.230
	H	10	-0.003
	H	11	-0.003
	H	12	0.023

	H	13	-0.024
	H	14	0.002
	H	15	-0.022
	H	16	0.005
	Cl	17	0.171
IM_{2-6}	N	1	0.037
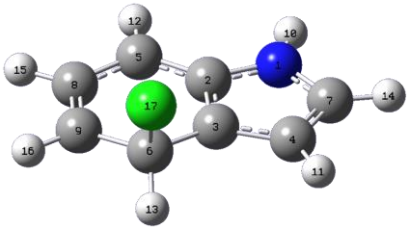	C	2	-0.217
	C	3	0.235
	C	4	-0.041
	C	5	0.612
	C	6	-0.098
	C	7	0.146
	C	8	-0.261
	C	9	0.481
	H	10	-0.002
	H	11	0.001
	H	12	-0.025
	H	13	0.024
	H	14	-0.007
	H	15	0.006
	H	16	-0.022
	Cl	17	0.130
C_8H_6N	N	1	0.256
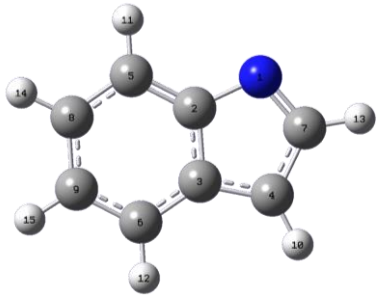	C	2	-0.021
	C	3	-0.147
	C	4	0.690
	C	5	-0.018
	C	6	0.270
	C	7	-0.101
	C	8	0.187
	C	9	-0.072
	H	10	-0.027
	H	11	0.000

H	12	-0.009
H	13	0.000
H	14	-0.009
H	15	0.001

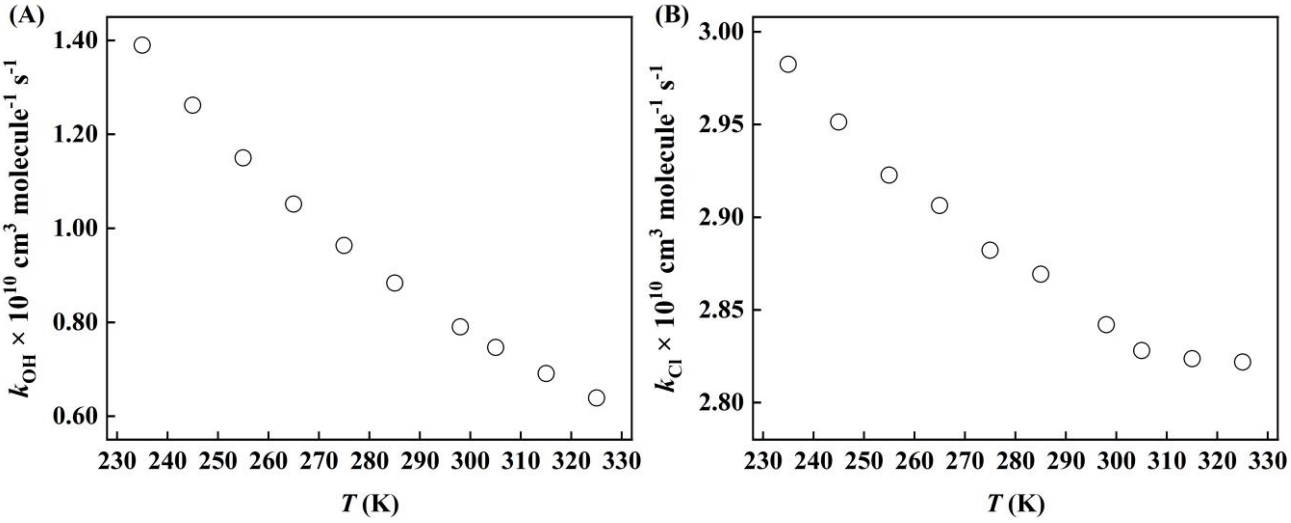

Figure S1. Calculated reaction rate constants (*k*) at 1 atm and over the temperature range from 230 to 330 K for the indole + ·OH (A) and indole + ·Cl (B) reactions.

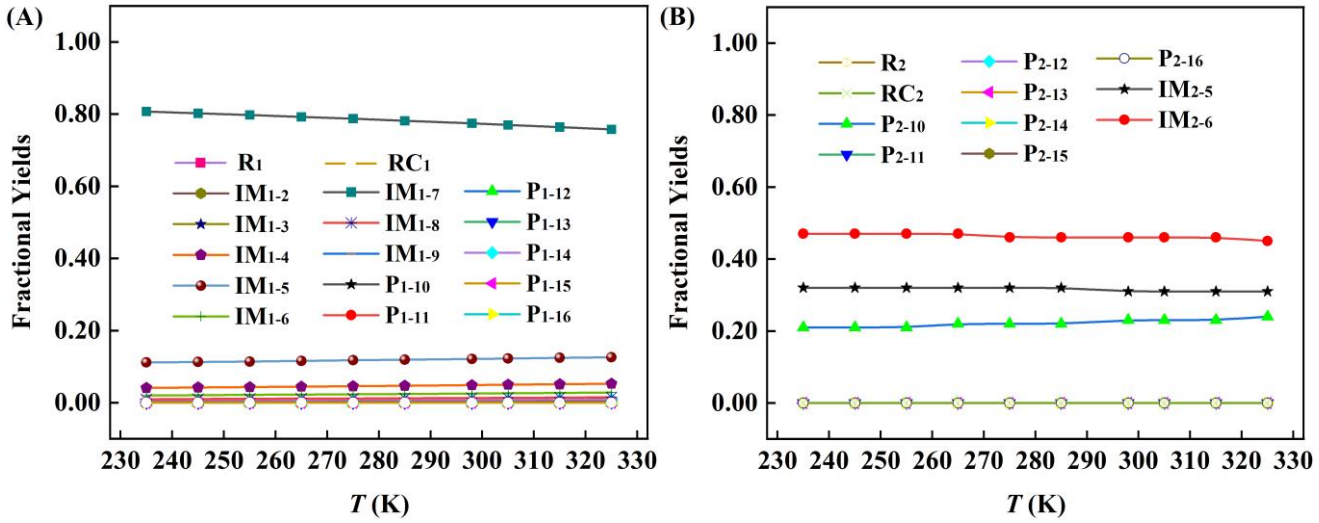

Figure S2. Calculated branching ratios (*Γ* values) at 1 atm and over the temperature range from 230 to 330 K for the indole + ·OH (A) and indole + ·Cl (B) reactions.

90

References

1. Guo, X. R.; Ma, F. F.; Liu, C., Niu, J., He, N., Chen, J. W.; Xie, H. B.: Atmospheric Oxidation Mechanism and Kinetics of Isoprene Initiated by Chlorine Radicals: A Computational Study, *Sci. Total Environ.*, 2020, 712, 136330.

2. Ma, F.F.; Xie, H. B.; Li, M.; Wang, S.; Zhang, R. Y.; Chen, J. W.: Autoxidation Mechanism for Atmospheric Oxidation of Tertiary Amines: Implications for Secondary Organic Aerosol Formation, *Chemosphere*, 2021, 273, 129207.

3. Xie, H. B.; Ma, F. F.; Wang, Y. F.; He, N.; Yu, Q.; Chen, J. W. Quantum Chemical Study on ·Cl-Initiated Atmospheric Degradation of Monoethanolamine. *Environ. Sci. Technol.* 2015, *49*, 13246-13255.

4. Xie, H. B.; Ma, F. F.; Yu, Q.; He, N.; Chen, J. W. Computational Study of the Reactions of Chlorine Radicals with Atmospheric Organic Compounds Featuring NH*x*-pi-Bond (*x*=1, 2) Structures. *J. Phys. Chem. A* 2017, *121*, 1657-1665.

5. NIST Computational Chemistry Comparison and Benchmark Database. NIST Standard Reference Database Number 101, R. D. Johnson III, Release 16a, August 2013. http://cccbdb.nist.gov/.